PHYSICAL REVIEW A VOLUME 36, NUMBER 10 NOVEMBER 15, 1987

Profiles of $(3/2)\omega_0$ emissions from laser-produced plasmas

B. K. Sinha and S. R. Kumbhare
Laser Division, Bhabha Atomic Research Centre, Bombay 400 085, Maharashtra, India

G. P. Gupta
Plasma Physics Division, Bhabha Atomic Research Centre, Bombay 400 085, Maharashtra, India
(Received 10 September 1986; revised manuscript received 28 April 1987)

Theoretical profiles of $(3/2)\omega_0$ emissions from laser-produced carbon plasmas, at plasma temperatures varying from 600 to 250 eV, corresponding to laser intensities varying from 1.5×10^{14} to 1.7×10^{13} W/cm^2 have been calculated. The peak shifts of these emissions have been compared with the experimental results obtained using a 1.0641-μm Nd:glass laser and they are found to be in good agreement. Theoretical estimates of wavelength shifts taking into account the variation of plasmon wave number have also been compared with the experimental values. Profiles of $(3/2)\omega_0$ emissions from planar slab targets of carbon, aluminum, and copper have been reliably measured and are compared with the theoretical estimates. Experimental results strongly suggest the saturation of two-plasmon–decay convective instability.

I. INTRODUCTION

With the appearance of the works of Bychenkov *et al.*[1,2] experimental studies of $(3/2)\omega_0$ emissions from laser-produced plasmas, from targets of different shapes and sizes, have generated a new incentive for the investigations of line shifts of these emissions from the exact $(3/2)\omega_0$ harmonic and the broadening of the lines due to the intrinsic nonlinear plasma interaction process as well as the Doppler effect, if any, caused by the freely expanding plasma. It is well known that, at one quarter of critical density n_c, both two-plasmon decay and stimulated Raman scattering (SRS) instabilities compete with each other to excite plasmons with frequency close to $\omega_0/2$, where ω_0 is the frequency of the incident light. The incident or reflected photons couple with an $\omega_0/2$ plasmon and this coupling is responsible for emissions of radiation with frequencies close to $\omega_0/2$ or $3\omega_0/2$. Observations of half- and three-halves harmonic emission have been variously reported by various authors, using different target geometries and different lasers of various wavelengths and pulse durations.[3–9] Stimulated Raman scattering, at the quarter critical surface, has been attributed to produce the second-harmonic emissions. However, a double peak structure of the $\omega_0/2$ spectrum, similar to that observed in the case of $3\omega_0/2$ emissions, strongly suggests $2\omega_p$ decay as the process responsible for the second-harmonic generation.[10–12] This observation is also supported by the lower threshold of the two-plasmon decay instability.[13–17] Kutty and Sinha,[18] for the case of stimulated Raman side scattering, using an exponential density profile, observed that this threshold is a strong function of density gradient scale length L. For L having the values of 100, 10, and 5 μm they estimated the threshold at around 1.14×10^{13}, 0.30×10^{14}, and 7.65×10^{14} W/cm^2, respectively. Hence, for larger values of L, SRS may also compete with two-plasmon–decay instability.

Although quite a good number of experimental and theoretical results have appeared on $(3/2)\omega_0$ emissions,[1,2,5,10,12,19–22] still the experimental data are not quantitative enough to give a well-defined conclusion about the shifts of these emissions from the exact $(3/2)\omega_0$ harmonic as well as the broadening of the lines as a function of the plasma parameters. The line shifts and the line broadening are two important experimentally observable parameters that are produced by the nonlinear laser-plasma interaction process and provide important clues as to what is happening inside the transient plasmas. Unfortunately, in-depth theoretical studies on $(3/2)\omega_0$ emissions are lacking. Avrov *et al.*[5] used a model where the plasmon wave number is the one which gives the maximum growth rate for two-plasmon–decay instability,[23] but does not necessarily allow for phase matching with an incident photon. Barr[19] has also, from brief theoretical considerations, given the wavelength from the exact $(3/2)\omega_0$ harmonic for a 1.06-μm laser. Bychenkov *et al.*[1,2] have given a detailed theory of $(3/2)\omega_0$ emission from laser-produced plasmas and our theoretical analysis is based on their earlier formulations; measurements of peak shifts from planar slab targets of carbon agree reasonably well with the theoretical estimates of Bychenkov *et al.*[1,2] Kartunnen's deductions[22] are also quite interesting, as he has taken into account the variation of plasmon wave number, while it propagates from the $2\omega_p$ region to the region of $(3/2)\omega_0$ generation.

In the present work theoretical profiles of $(3/2)\omega_0$ emissions from laser-produced carbon plasma at different laser intensities have been obtained and compared quantitatively with the experimental results. Supplementary data on the profiles of $(3/2)\omega_0$ emission from planar slab targets of aluminum and copper are also discussed. The reliability of temperature estimation from peak shifts of these emissions has been examined for s-polarized pump wave. At higher laser intensities strong evidence of

two-plasmon saturation is indicated. Analysis on the basis of Kartunnen's theoretical deductions suggests a way to study the variation of the plasmon wave number from the origin of $2\omega_p$ generation to the point of $(3/2)\omega_0$ emission. This variation has been approximately estimated.

II. THEORY

Generally, the pump wave combination scattering on the parametrically excited Langmuir oscillations near quarter critical density layer is responsible for the generation of $(3/2)\omega_0$ emissions in the laser-produced plasmas. Three-plasmon coupling is also a distinct possibility but this is generally regarded as a higher-order process.[5] Its probability was evaluated by Alexandrov[24] who reported that the three-plasmon coupling contribution to the $(3/2)\omega_0$ emission is negligibly small under the laser-produced plasma conditions. Moreover, Langmuir oscillation parametric excitation may also be caused by stimulated Raman scattering. However, as reported in Sec. I, the two-plasmon instability threshold is observed to be lower than that of SRS (Refs. 13–15) if the plasma density gradient scale length L, near the $n_c/4$ layer, is not too large so that the following inequality holds true:

$$(k_0 L)^{1/6} < c/V_{T_e} , \tag{1}$$

where $k_0=(\omega_0/c)$ pump wave number. For typical experimental conditions $k_0 L < 10^2-10^3$, $T_e \sim 0.5$ keV and, consequently, the inequality, as expressed by Eq. (1), is valid. Thus, SRS contribution to the harmonic generation may be neglected.

A. Peak shifts from exact $(3/2)\omega_0$ harmonic

Avrov *et al.*[5] considered a model, in which the plasmon wave number which has the highest growth rate for the two-plasmon decay was used,[23] but the model had the limitation that it did not necessarily allow for phase matching with the incident radiation. This model gave

$$\Delta\lambda p = -22.7 T_e \cos\theta \ (\text{Å}) , \tag{2}$$

where $\Delta\lambda_p$ is the wavelength shift from exact $(3/2)\omega_0$ harmonic, T_e is the electron temperature in keV, and θ is the angle of scattered light with respect to the incident laser light.

Barr[19] considered phase matching between an incident photon and $2\omega_p$ generated plasmon adding together to form $(3/2)\omega_0$ radiation. It was noted that the forward scattered plasmon must have a wave number which is small compared to the wave number which is expected near threshold.[23] For a 1.06-μm laser, Barr gave the wavelength shift from the exact harmonic as

$$\Delta\lambda_p = -33.9 T_e(\cos\theta - 0.919) \ \text{Å} . \tag{3}$$

Bychenkov *et al.*[2] considered, in detail, an obliquely incident laser light on the plasma (Fig. 1) and, using the reported formulations of Bychenkov *et al.*,[1] connected the harmonics generation with the two-plasmon convective instability at the quarter critical density layer. They noted that harmonic spectra and intensities essentially

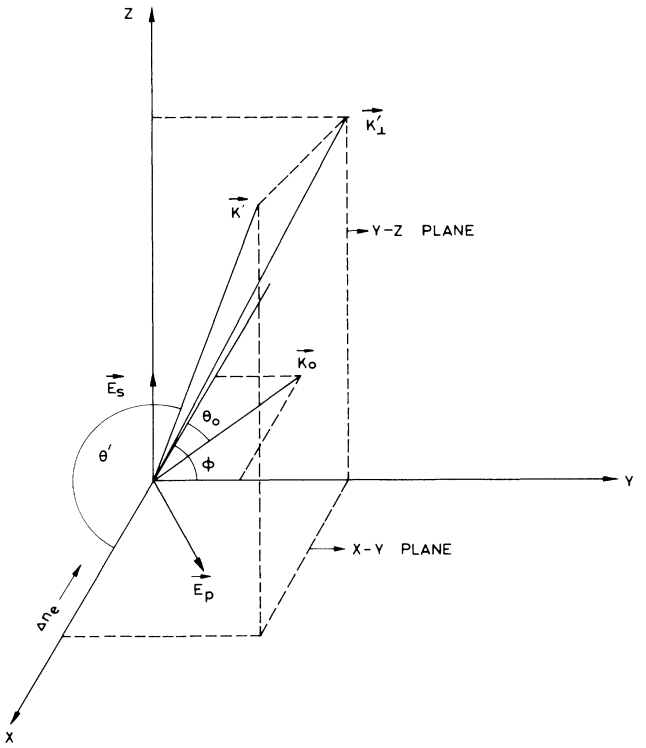

FIG. 1. Arrangement of wave vectors of the obliquely incident and scattered waves to and from an inhomogeneous plasma; $\mathbf{E}_s$ and $\mathbf{E}_p$ represent s and p components of the pump wave electric field.

depend on the pump wave polarization. Using the formulations of Bychenkov *et al.*,[1] Bychenkov *et al.*[2] arrived at the expression for the scattered wave energy flux spectral density as (Fig. 1)

$$q'(\omega',\mathbf{n}') = \frac{e^2}{2\pi m^2 c^5} \frac{L q_0 \cos\theta_0 \, |\mathbf{k}'-\mathbf{k}_0|}{[(\frac{3}{4})-\sin^2\theta_0]^{1/2} \, |k_x'|} \times W_l(\omega'-\omega_0, \mathbf{k}_\perp'-\mathbf{k}_{0\perp}, x_g) \left[\frac{\omega'}{\omega_0}\right]^3 , \tag{4}$$

where ω' is the scattered wave frequency, $\mathbf{n}'$ is the unit vector along the scattered direction, q_0 is the pump wave energy density flux in vacuum, θ_0 is the pump wave incidence angle, $\mathbf{k}'=(\mathbf{k}_{0x},\mathbf{k}_{0\perp})$ is the scattered wave vector in the harmonics generation region, $\mathbf{k}_0=(\mathbf{k}_{0x},\mathbf{k}_{0\perp})$ is the pump wave vector in the harmonics generation region, $\mathbf{k}_x',\mathbf{k}_{0x}$ are the vector components along density inhomogeneity direction, $\mathbf{k}_\perp',\mathbf{k}_{0\perp}$ are the vector components perpendicular to the density inhomogeneity direction, W_l is the Langmuir wave energy flux spectral density, and x_g is the coordinate of the harmonic generation region.

For an s-polarized light, under the normal pump wave incidence, they gave the approximate expression for the peak shift $\Delta\lambda_{ps}$ from the exact $(3/2)\omega_0$ harmonic, as

$$\Delta\lambda_{ps\pm}=\mp\tfrac{2}{3}\lambda_0\left[\frac{(\frac{2}{3})y}{1\pm(\frac{2}{3})y}\right],$$
$$y=\tfrac{9}{8}\left[\frac{V_{T_e}}{c}\right]^2(1+12\sin^2\theta')^{1/2}, \tag{5}$$

where V_{T_e} is the thermal velocity of electrons, c is the velocity of light, and θ' is the scattering angle measured with respect to the incident beam.

For a p-polarized light they also gave an expression for the maximum possible shift $\Delta\lambda_{ppm}$ determined by Landau damping as

$$\Delta\lambda_{ppm}\approx\tfrac{1}{3}\lambda_0\left[\frac{V_{T_e}}{c}\right][(\tfrac{3}{4})-\sin^2\theta_0)]^{1/2}, \tag{6}$$

where θ_0 is the angle of incidence that the pump wave makes with the direction of density gradient scale length change.

Kartunnen[22] considered the variation of plasmon wave number from a $2\omega_p$ region to the region of $(3/2)\omega_0$ generation and, for a red shift, due to interaction between the red plasmon and the incident photon $(\mathbf{k}_0,\omega_0)$; he approximately deduced the expression as

$$\Delta\lambda_p=\frac{1}{2}\left[\frac{V_{T_e}}{c}\right]^2\lambda_0\left[1+\frac{2}{\sqrt{3}}(11\alpha^2-8\sin^2\theta'-4\sqrt{6}\alpha^2\cos\theta')^{1/2}\right], \tag{7}$$

where $\alpha=k_2/k_2'$ is the measure of change in the plasmon wave number from the $2\omega_p$ region (k_2) to the region of $3\omega_0/2$ generation (k_2'). The symbols k_2 and k_2' represent associated plasmon wave numbers in the two regions. For the parallel density gradient ($\nabla n\|\mathbf{k}_0$) the red plasmon $(\mathbf{k}_2,\omega_2)$ travels down the gradient indicating that the two-plasmon decay operates at higher or equal density than the $3\omega_0/2$ region. This means that we have $\alpha\leq 1$ in Eq. (7). We have considered various values of α for the analysis of our results in Sec. V.

B. Intrinsic profile of $(3/2)\omega_0$ emissions

We have defined the intrinsic profile of $(3/2)\omega_0$ emissions as the profile obtained as a result of differential convective amplification coefficient of the Langmuir wave two-plasmon instability as a function of frequency of the scattered radiation. With reference to Eq. (4), one obtains

$$|\mathbf{k}'-\mathbf{k}_0|=[(\mathbf{k}'-\mathbf{k}_0)\cdot(\mathbf{k}'-\mathbf{k}_0)]^{1/2}. \tag{8}$$

The scattered wave number k' is obtained from the corresponding dispersion relation

$$(\omega')^2=\omega_p^2+c^2k'^2, \tag{9}$$

where ω_p is the plasma frequency.

In order to calculate the scattered energy flux density, one should know the amplified plasmon energy flux density. The theory for this is still far from complete[2] because one does not know exactly which parametric process results in amplification and how far from the origin of the plasmons the nonlinear phase-matching condition is satisfied, giving rise to harmonic generation. Assuming that the harmonic generation takes place near the threshold region and the parametric instability saturation is of convective nature, the Langmuir energy flux density can be written as[2,25]

$$W_l(\omega,\mathbf{k}_\perp)=\frac{n_0KT_e}{n_0\lambda_D^3}\exp[2\chi(\omega,\mathbf{k}_\perp)], \tag{10}$$

where $\chi(\omega,\mathbf{k}_\perp)$ is the Langmuir-wave two-plasmon instability convective amplification coefficient, K is the Boltzmann constant, λ_D is the Debye wavelength, and n_0 is the electron density.

The temperature T_e determines the thermal fluctuation level. If the plasma density linearly depends on the coordinates x, then $\chi(\omega,\mathbf{k}_\perp)$ is determined from the relation[2]

$$\chi(\omega,\mathbf{k}_\perp)=\frac{\pi}{6}\frac{L}{|k_{0x}|V_{T_e}^2}\frac{(\mathbf{k}\cdot\mathbf{V}_E)^2(\mathbf{k}\cdot\mathbf{k}_0-k_0^2/2)}{k^2[(\mathbf{k}-\mathbf{k}_0)\cdot(\mathbf{k}-\mathbf{k}_0)]}, \tag{11}$$

where $\mathbf{V}_E$ is the electron oscillation velocity in the pump wave electric field and $\mathbf{k}=(\mathbf{k}_x,\mathbf{k}_\perp)$ is the amplifying plasmon wave vector. For normal incidence, $|k_{0x}|=k_0$. For no amplification, $\chi=0$ and Eq. (10) gives the usual thermal fluctuation wave energy density given by Nicholson.[25] The x component of the plasmon wave vector is determined by decay conditions and is obtained as

$$k_x=\frac{(\omega-\omega_0/2)\omega_0}{3k_0V_{T_e}^2}+\frac{k_0}{2}. \tag{12}$$

Using Eqs. (10)–(12), one obtains the Langmuir wave energy density in terms of scattered electromagnetic parameters as

$$W_l(\omega'-\omega_0,\mathbf{k}_\perp')=\frac{n_0KT_e}{n_0\lambda_D^3}\exp 2\chi(\omega'-\omega_0,\mathbf{k}_\perp'). \tag{13}$$

The corresponding amplification coefficient and the value of k_x, after replacing ω by $(\omega'-\omega_0)$ in Eqs. (11) and (12), are obtained as

$$\chi(\omega'-\omega_0,\mathbf{k}_\perp)=\chi_{max}\left[\frac{k_\perp'^2(2k_x-k_0)^2}{(k_x^2+k_\perp'^2)[k_0^2+k_\perp'^2+k_x(k_x-2k_0)]}\right], \tag{14}$$

where

$$\chi_{max}=\frac{\pi}{24}\frac{V_E^2}{V_{T_e}^2}k_0L\cos^2\theta, \tag{15}$$

$$k_x=\frac{(\omega'-3\omega_0/2)}{3k_0V_{T_e}^2}+\frac{k_0}{2}. \tag{16}$$

The symbol θ represents the angle between $\mathbf{k}_\perp'$ and $\mathbf{V}_E$. For the experimental situation as shown in Fig. 2, the angle θ is given by $\pi/4$. The energy flux density of scat-

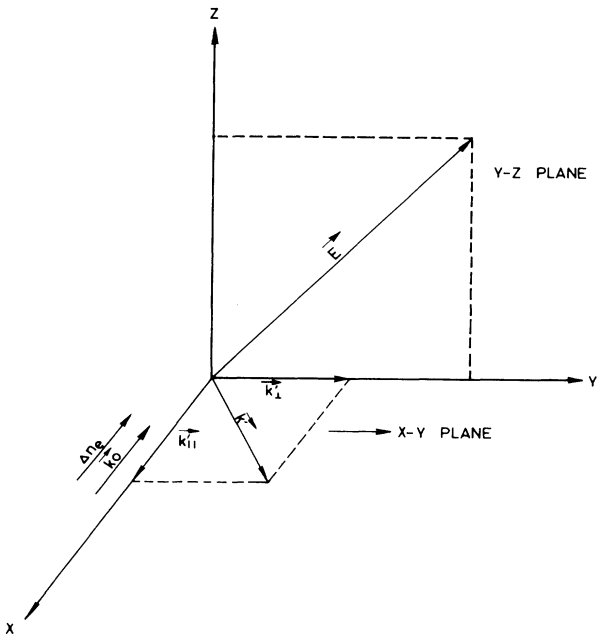

FIG. 2. Vectorial representation of the experimental situation for normal incidence. The incident, scattered, and polarization vectors are clearly shown.

tered radiation has been studied using Eqs. (4), (9), and (13)–(16) and the results are discussed in Sec. IV.

III. THE EXPERIMENTS

Figure 2 vectorially represents the experimental situation. The directions of the incident beam and plasma density inhomogeneity are shown by the symbols $\mathbf{k}_0$ and Δn_e. The direction of scattering is represented by the symbol $\mathbf{k}'$, which is in the incident plane and makes an angle $\pi/4$ with the positive x direction. The components $\mathbf{k}'_{\parallel}$ and $\mathbf{k}'_{\perp}$, parallel and perpendicular to the positive x direction, are also shown. The vector $\mathbf{E}$ represents the direction of polarization of the incident beam. The plasma is formed at the origin of the rectangular coordinate system.

Experiments were conducted using 20 J–5 nsec, 1.0641-μm Nd:glass laser amplifier system, with a Nd:YAG oscillator (where YAG is yttrium aluminum garnet) on planar slab targets of carbon, aluminum, and copper. The linewidth of the incident beam was measured to be 4.5 Å. Originally the light was p polarized but the plane of vibration of E was rotated by an angle $\pi/4$ by the Faraday isolator which was positioned between the laser chain and the plasma chamber. As a result, the plane of vibration of E made an angle of $\pi/4$ with the incident plane, giving equal components in both the s- and p-polarization directions. The detector system consisted of a Pacific Instruments Incorporated MP 1018 B grating monochromator, coupled with an RCA-7265 photomultiplier tube with an S-20 response, and a Tektronix 7834 storage oscilloscope. The grating monochromator uses a Jarell Ash plane reflection replica diffraction grating in Czerney Turner configuration and has a reciprocal linear dispersion, at exit slit of 17.5 Å/mm, in the first order, with 1180 lines/mm grating, which was used in the present experiment. The monochromator was calibrated using standard light sources of a He-Ne laser, Hg(I), Hg(II), Ne, and a hollow potassium cathode at the wavelengths 6328, 7300, 5790.7, 7032.4, and 7664.9 Å, respectively, and the wavelength of scattered radiation was measured with an accuracy of ± 1 Å. The monochromator gave a satisfactory performance. Shot-to-shot variation in laser energy was found to be within $\pm 5-10\%$ and the focal spot was measured with an accuracy of $\pm 7\%$. This gave the accuracy of laser intensity measurements within $\pm 25\%$. X-ray diagnostics using absorption filters and the two-foil ratio technique gave the electron temperature which was found to be in reasonably good agreement with the results of Kang *et al.*[26] and Sakabe *et al.*[27] who quoted the results of other works also. The results quoted by Sakabe *et al.*[27] usually show a scatter of 10–15% in temperature values. Within the scatter our measurements were found to be reasonable. The method and reliability of the technique have already been reported in Sinha[28] and Sinha and Gopi.[29] The main source of experimental error was found to be the fluctuation in laser intensity and the focal spot size. From the results of Kang *et al.*[26] and also from Sakabe *et al.*,[27] the scaling of plasma temperature on laser intensity can be taken between $\phi^{2/9}$ to $\phi^{4/9}$. Therefore, error in temperature estimation due to the lower scaling factor on ϕ comes to within approximately 6–11%. Reflection losses from the optical components were duly taken into account while estimating the values of laser intensity. An aspheric f/1.33 lens was used to focus the beam onto the target. Intensity measurements in the focal plane showed no significant variation; hence, the temperature measurements were found to be reliable within the experimental bars. Emission from plasma, at wavelengths of interest, consisted of a broad pulse of 20–25 nsec full width at half maximum (FWHM) pulse width due to the background radiation over which much narrower pulses from the harmonics were superimposed. The contribution due to background radiation was approximately constant in the wavelength region of investigation, though it was different at different laser intensities. This contribution was measured on both ends of the line profile and its values were checked for each set of the experiments.

IV. THEORETICAL AND EXPERIMENTAL RESULTS

Langmuir wave two-plasmon instability convective amplification coefficient χ is plotted in Figs. 3(a)–3(c) as a function of the shift $\Delta\lambda$ of scattered radiation from λ_0(7094 Å) at the temperatures of 600, 520, 480, and 250 eV for carbon plasma corresponding to the laser intensities of 1.5×10^{14}, 8.0×10^{13}, 4.1×10^{13}, and 1.7×10^{13} W/cm^2, respectively. Equation (14) was used to estimate the value of χ. The values of plasma temperature and the laser intensity were taken for the convenience of interpreting the experimental results. One notes that the value of $\Delta\lambda_p$, at which the peak of each curve occurs, shifts towards the origin for descending values of tem-

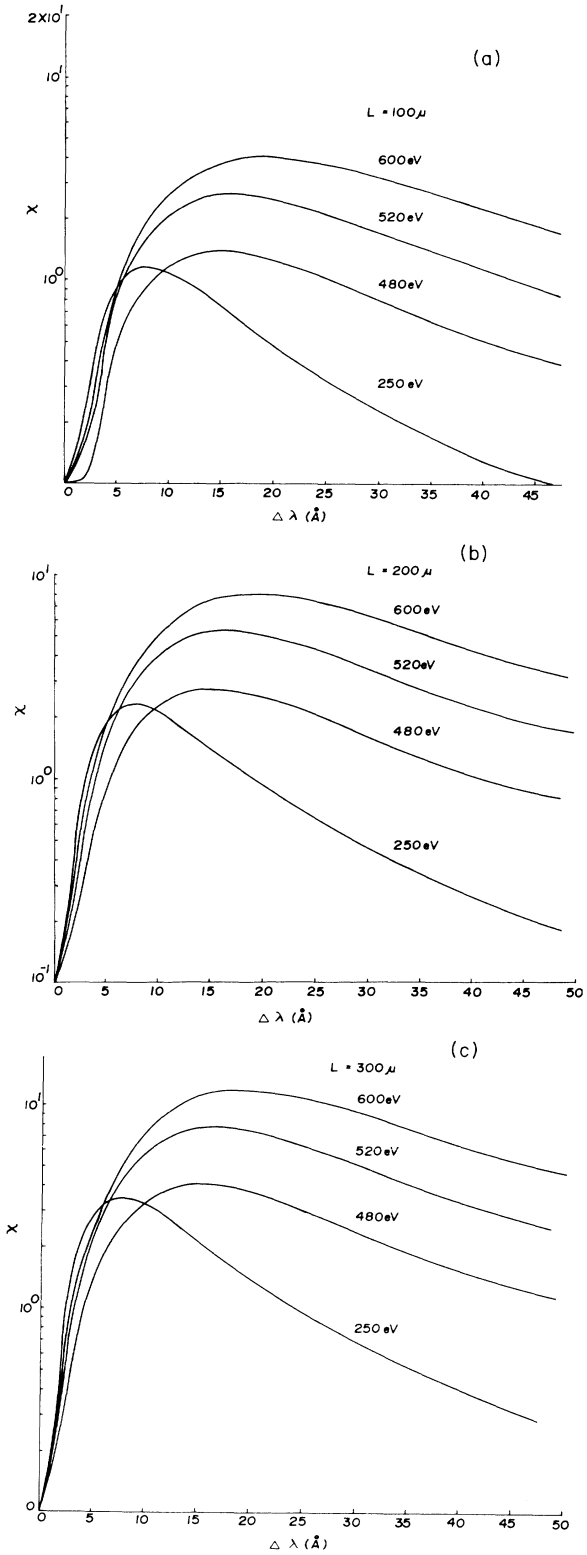

FIG. 3. (a) Two-plasmon convective amplification coefficient χ as a function of $\Delta\lambda$ for different plasma temperatures and laser intensities and for $L=100$ μm. Here $\Delta\lambda=(\lambda'-\frac{2}{3}\lambda_0)$. (b) Two-plasmon amplification coefficient χ as a function of $\Delta\lambda$ for $L=200$ μm. (c) Two-plasmon amplification coefficient χ as a function of $\Delta\lambda$ for $L=300$ μm.

perature. Moreover, the value of χ is not symmetrical around its peak but has similar profiles on both sides of the Y axis. The curve rises fast, reaches the peak, and then decreases comparatively slowly. The amplification coefficient vanished at $\Delta\lambda=0$, that is, at $\lambda'-\frac{2}{3}\lambda_0=0$, which is obvious from Eqs. (14) and (16). At $\omega'=(3/2)\omega_0$, $k_x=k_0/2$; hence, χ becomes zero at $(3/2)\omega_0$ from relation (14). The value of W_l [Eq. (13)] is very sensitive to the value of χ. From Figs. 3(a)–3(c) one notes that the values of $\Delta\lambda_p$ at which the peak of χ profiles occurs, at a given temperature, are independent of the values of L, which have been taken as 100, 200, and 300 μm to illustrate this point. This is obvious from Eq. (11) in which the second term of the numerator determines the value of $\Delta\lambda$ at which the peak of the χ profile occurs. Limitations of Eq. (13) are discussed in the subsequent section on profile broadening.

The value of n_0, for calculations, has been taken as 2.5×10^{20} which is the $n_c/4$ value of the plasma produced by glass laser. Three values of L have been taken as shown in Figs. 3(a)–3(c) and 4(a)–4(d). Herbst *et al.*,[30] using a 3–5-nsec, Nd:glass laser, at a laser intensity of 7×10^{12} W/cm^2, measured the density profile of an aluminum plasma. Taking into account the errors reported in the experiment, the density gradient scale length, at $n_c/4$, can be estimated to be in the range of 150–200 μm. Therefore, we have found it convenient to consider three values of L. Moreover, at this stage it is useful to check the inequality expressed by Eq. (1). Taking $T_e=500$ eV, λ_0 is the wavelength of incident light equal to 1.0641 μm and $L=100$, 200, and 300 μm, the right-hand side of the inequality comes out to be 32.02 and the left-hand side of the inequality comes out to be 2.897, 3.252, and 3.479 for $L=100$, 200, and 300 μm, respectively. For lower temperature this inequality is still better satisfied. Therefore, the inequality is well satisfied and one may ignore the contribution due to SRS. As far as the error in the estimation of peak shift due to the error in the value of L is concerned, the approximate peak shift as given by Eq. (5) does not depend on the value of L and the exact peak shift from profile calculations based on Eqs. (13), (14), and (15) is governed by the term $(2k_x-k_0)^2$ in the numerator of Eq. (14). Therefore, error in the estimation of L will not cause any error in the estimation of the peak shift which can be noted from the data presented in Table I.

Figures 4(a)–4(d) display the plot of the coefficient of the conversion of pump radiation into the harmonic radiation (q'/q_0) for carbon plasma, where q_0 is the pump energy-flux density, for four values of laser intensities and their estimated corresponding temperatures. One notes that each curve is approximately symmetrical around the peak in the vicinity of the FWHM value of the linewidth. The FWHM value $\Delta\lambda_B$ of the linewidth of each curve as well as the peak shift $\Delta\lambda_p$ have been shown in Figs. 4(a)–4(d) by horizontal and vertical lines, respectively. The linewidths $\Delta\lambda_B$, as shown in Figs. 4(a)–4(d), vary approximately between 5–10 Å for different values of laser intensities and their corresponding temperatures and different values of L. The profiles are much sharper as compared to those of experimental

measurements. The values of the peak shift are independent of the values of L and they are tabulated in Table I. These theoretical profiles of $(3/2)\omega_0$ emission are exact and are plotted on the basis of Eqs. (4) and (13)–(16). The peak shifts obtained from these profiles are exact, whereas those obtained from Eq. (5) are approximate.

Figure 5 shows the relative signal in volts as a function of wavelength for a carbon plasma at laser intensities of 1.5×10^{14}, 8.5×10^{13}, 4.1×10^{13}, and 1.7×10^{13} W/cm^2. The peaks of these profiles are shown by vertical lines. The profiles give linewidths of 93, 58, 28, and 15 Å at the four laser intensities in descending order. The profiles are approximately symmetrical and they get broader and broader at higher intensities. Figures 6 and 7 display similar profiles for aluminum and copper and the relevant numerical values are also shown. The flat

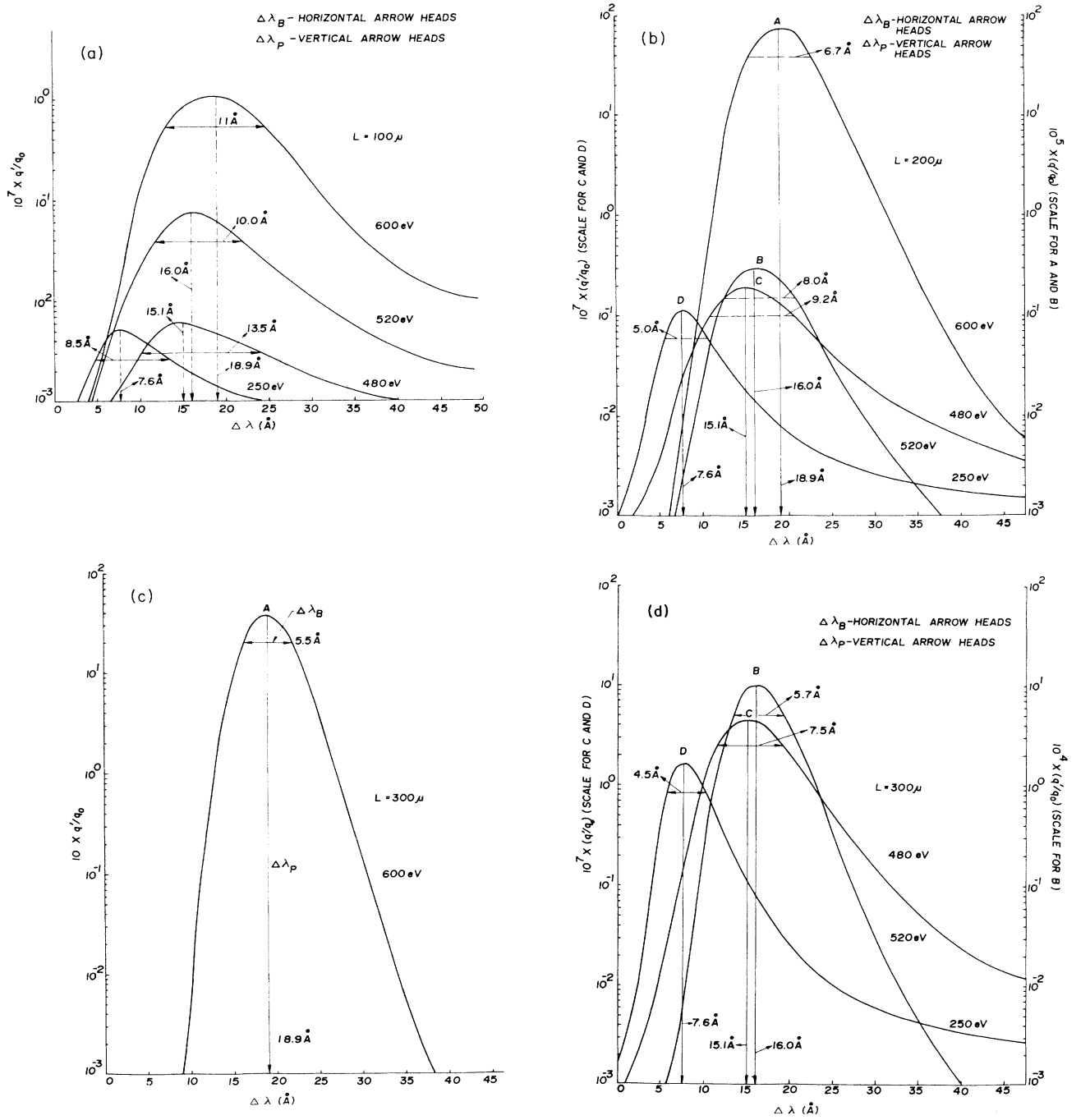

FIG. 4. (a) Variation of coefficient of conversion of pump radiation into the harmonic radiation (q'/q_0) as a function of $\Delta\lambda$ at different laser intensities and temperatures for carbon. $L=100$ μm. (b) Variation of coefficient of conversion of pump radiation into the harmonic radiation (q'/q_0) with $\Delta\lambda$ for $L=200$ μm. (c) Variation of (q'/q_0) with $\Delta\lambda$ for $L=300$ μm and $T_e=600$ eV. (d) Variation of (q'/q_0) with $\Delta\lambda$ for $L=300$ μm and $T_e=520$, 480, and 250 eV.

TABLE I. Data on theoretical and experimental estimate of peak shifts $\Delta\lambda p$'s for carbon.

Observation number	Measured temperature (eV)	Red shift (Å) A Experimental	B Bychenkov's works Approximate [Eq. (5)]	B Bychenkov's works Exact [Eqs. (4), (13)–(16)] ($L=100,200,300\mu$m)	C Kartunnen's works $\alpha=1.0$	C Kartunnen's works $\alpha=0.8$	C Kartunnen's works $\alpha=0.6$
1	600±60	15 ±1	16.3	18.9	22	17.3	11.6
2	550±55	14 ±1					
3	520±50	13 ±1	14.2	16.0			
4	480±45	10 ±1	13.3	15.1	17.6	13.8	9.3
5	450±45	13 ±1					
6	425±40	11 ±1					
7	400		10.9		14.7	11.5	7.7
8	360±35	8.8±1					
9	310±30	6.8±1					
10	300				11.0	8.6	5.8
11	275±30	7.5±1					
12	250±30	2 ±2	6.8	7.6	9.2	7.0	5.0

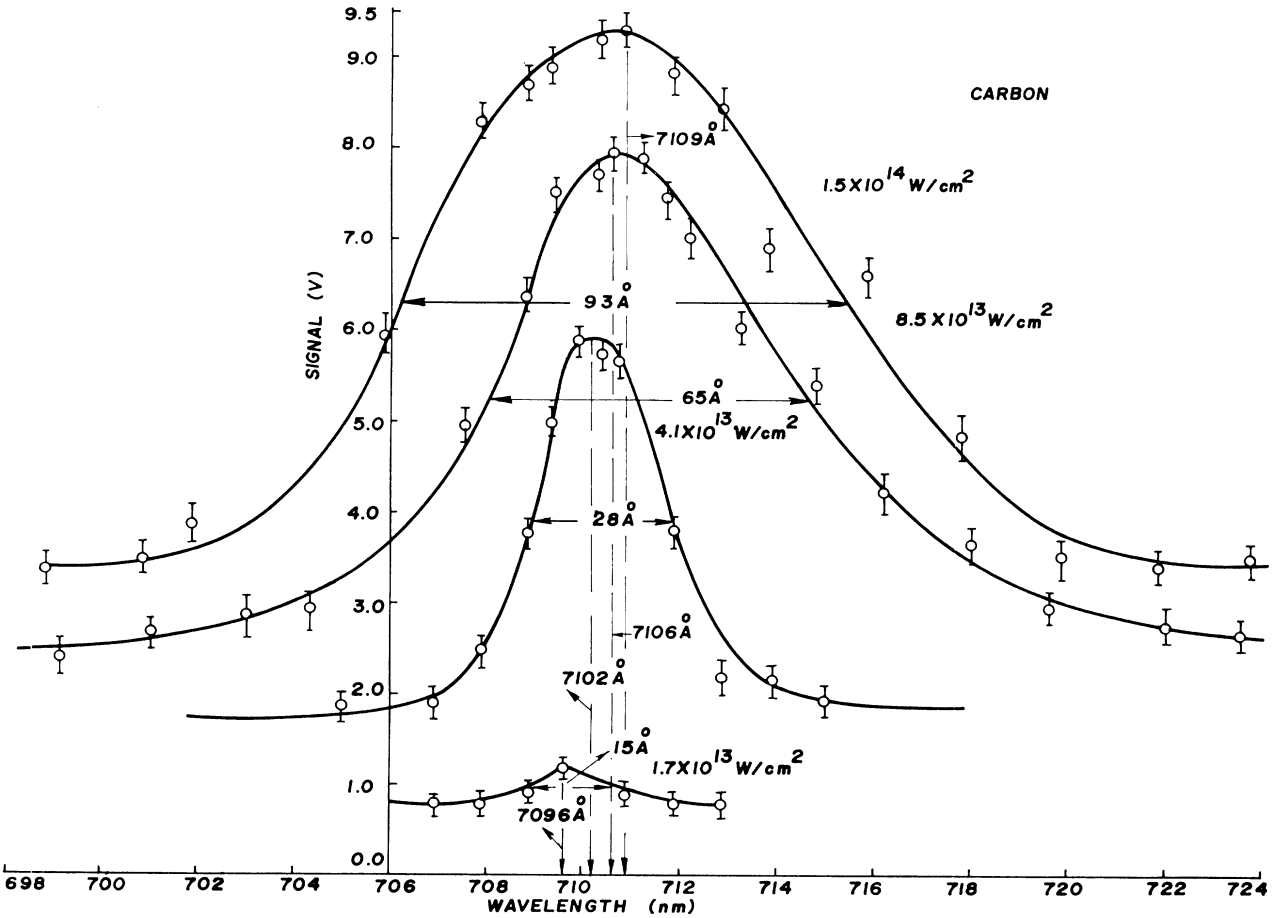

FIG. 5. Profiles of (3/2)ω_0 emissions for carbon plasma at different laser intensities as a function of $\Delta\lambda$.

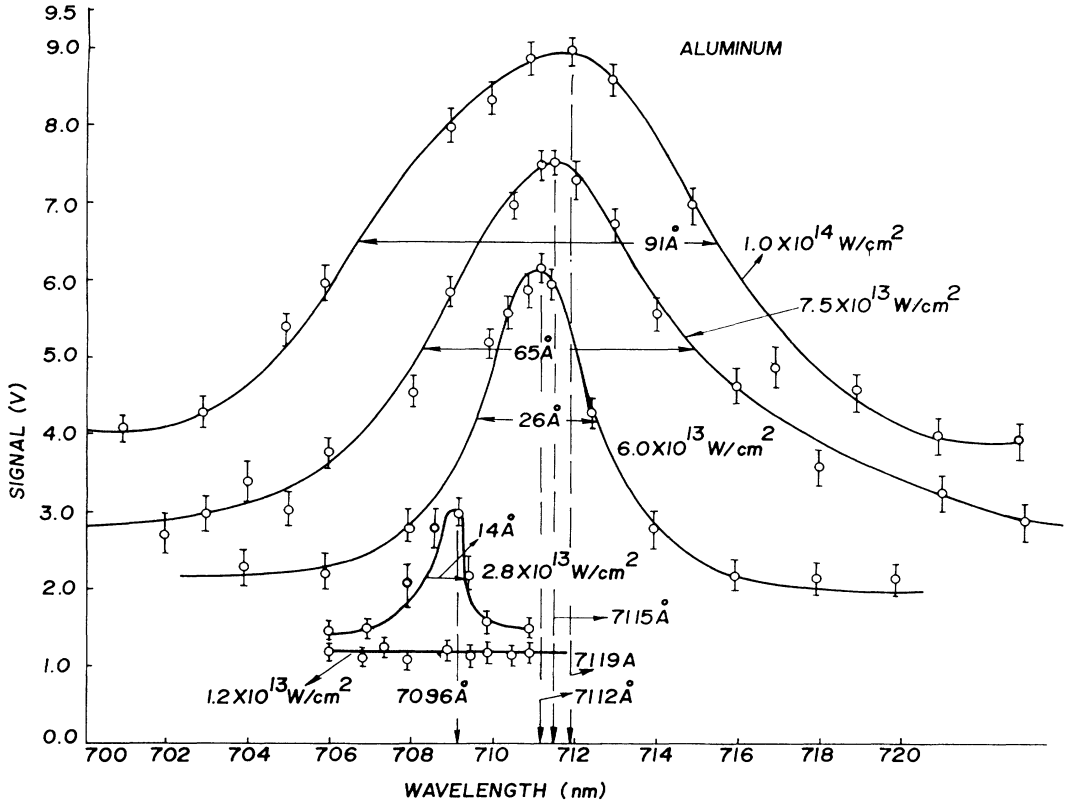

FIG. 6. Profiles of $(3/2)\omega_0$ emissions for aluminum plasma at different laser intensities.

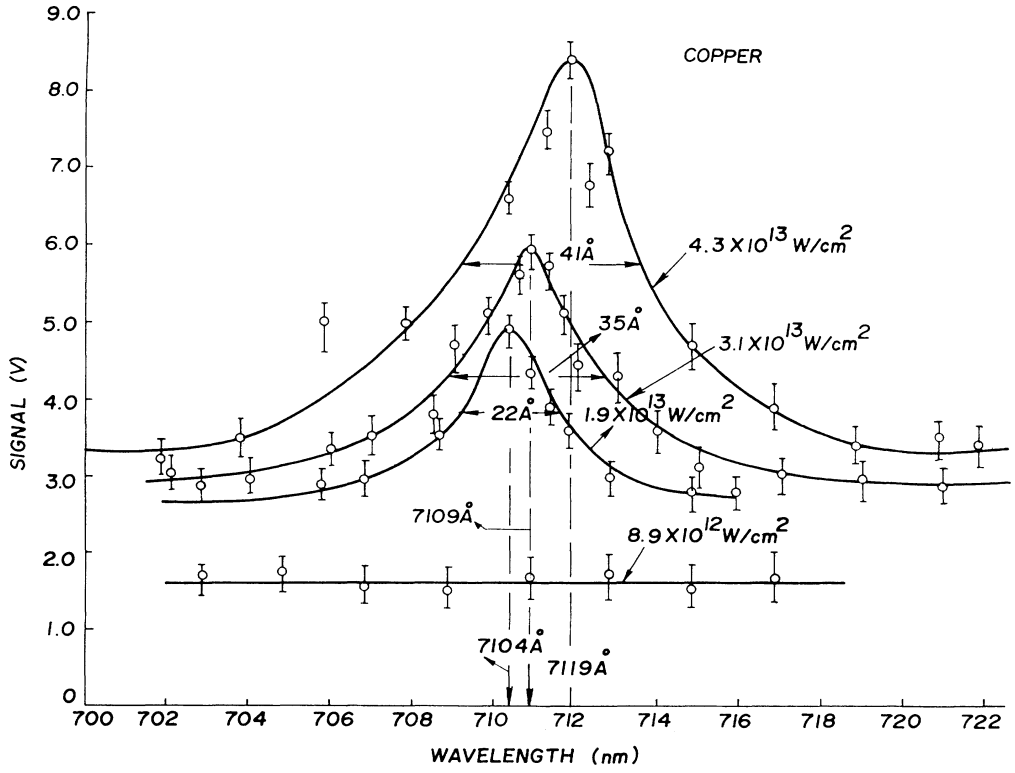

FIG. 7. Profiles of $(3/2)\omega_0$ emissions for copper plasma at different laser intensities.

lines show the occurrence of no signals. The supplementary data on aluminum and copper support the conclusions obtained from the data on the carbon plasma.

Figure 8 shows the experimental and theoretical values of the peak shift as a function of electron temperature for carbon plasma. The lines A_1 and A_2 represent the peak shifts estimated from Eqs. (4), (13)–(16), and from Eq. (5), respectively. Whereas line A_1 gives the exact peak shift, line A_2 gives the approximate one. The linear variations B_1, B_2, and B_3 are obtained from Eq. (7) for three values of α ($\alpha=1.0$, 0.8, and 0.6). The straight line C gives the best fit to experimental estimation of the peak shift at different temperatures. At a temperature of 250 eV, the experimental measurement of peak shift is a bit off the straight line C. This is because this measurement has been made almost at the threshold intensity for $(3/2)\omega_0$ emission and the signal height is very close to the background radiation and the error involved in this measurement is much higher than those involved in the measurements obtained at higher intensities. The results are discussed in Sec. V. The results obtained from Eqs. (2) and (3) usually fall far off the experimental values. Hence, they are not shown.

V. DISCUSSION

Although it is a bit difficult to establish the exact coupling mechanism responsible for the emission of $(3/2)\omega_0$ emission in solid target laser-plasma experiments,[1,2,5,8,11,13,20–22] we have tried in the present work quantitative studies of the profiles of $(3/2)\omega_0$ emissions on the basis of theoretical formulations presented by Bychenkov *et al.*[1,2] We have considered their work because they have taken into account the polarization of the pump wave in three dimensions. We have also considered the estimates of peak shifts on the basis of the formulation of Bychenkov *et al.*[1,2] and that of Kartunnen.[22] Firstly, it is interesting to look at the estimates of red shifts $\Delta\lambda_p$ of $(3/2)\omega_0$ emissions. The approximate theoretical estimates on the basis of the works of Bychenkov *et al.* [Eq. (5)] are presented and compared with those of the exact calculations based on Eqs. (4) and (13)–(16) and displayed in Figs. 4(a)–4(d) and experimental measurements. These values are also tabulated in Table I. We note that the straight lines A_2 and C closely agree with each other. But the values represented by A_2 are approximate. The values obtained from exact calculations are represented by the line A_1 and the experimental values represented by the line C are approximately within 10–15 % of the values represented by A_1. Considering the big scatter in temperature measurements[27] this agreement is reasonable. Moreover, as observed by Bychenkov *et al.*,[2] the theory for $(3/2)\omega_0$ is still far from complete, because one does not know exactly which parametric process results in amplification and how far from the origin of the plasmons the nonlinear phase-matching condition is satisfied giving rise to harmonic generation. However, Kartunnen[22] approximately considered the variation of the plasmon wave number from the point of origin to the point of $(3/2)\omega_0$ emission. The values represented by line B_1 do not agree with those of line c and this is expected because, for the line B_1, we have taken $\alpha=1.0$; that is, we have not considered the variation of the plasmon wave num-

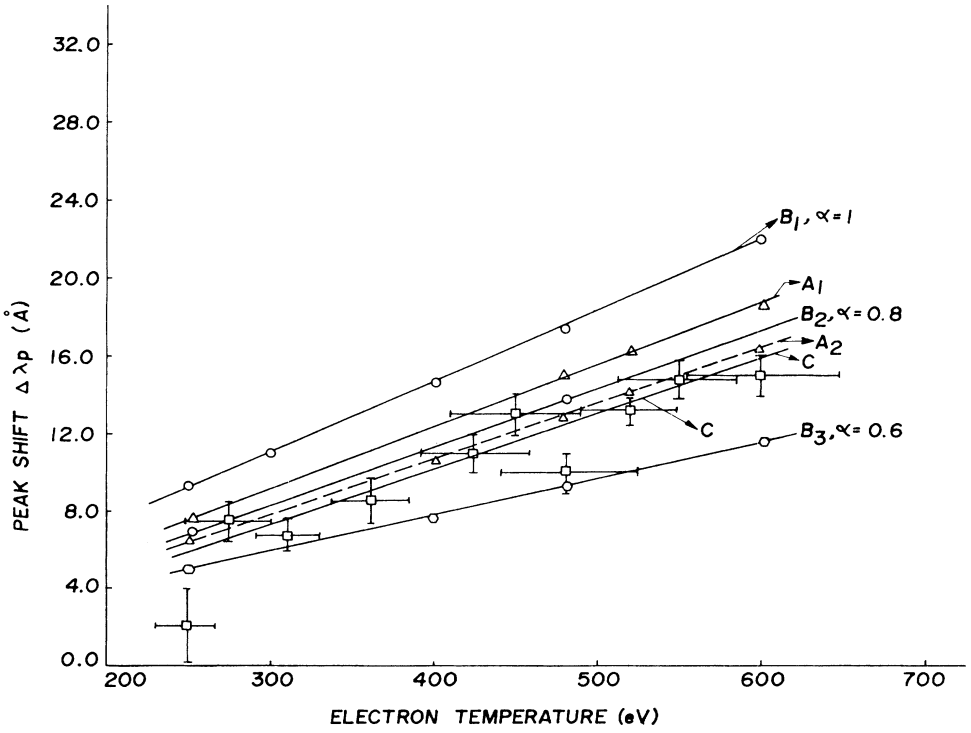

FIG. 8. Experimental and theoretical estimate of peak shift $\Delta\lambda_p$ as a function of temperature T_e.

ber. But if we consider the values represented by lines B_2 and B_3, estimated on the basis of $\alpha=0.8$ and 0.6, respectively, the values represented by line c fall in between those of B_2 and B_3. In fact, the experimental value is very close to the theoretical variation obtained when we take $\alpha=0.7$ (not shown in the figure). From this figure we conclude that it is necessary to know the exact estimate of the parameter α if we wish to estimate the electron temperature reliably using Eq. (7). Conversely, one can estimate the value of α if one knows the correct estimate of the temperature. Therefore, it is possible to study the plasma turbulence, which controls α, from the measurements of peak shifts of these emissions.

Secondly, it is interesting to consider the profiles of these emissions. From the sets of Figs. 5, 6, and 7 it is clearly noted that the linewidth of these emissions is much broader than the theoretical estimate as shown in Figs. 4(a)–4(d) and decreases sharply as the laser intensity decreases. Doppler-shifted profile calculations using Eqs. (4) and (13)–(16) at plasma expansion velocities of 10^7-10^8 cm/sec have shown insignificant contribution (2–3 Å) due to the Doppler effect to the broadening of the observed lines. Therefore, Doppler broadening is ruled out. Since the linewidth of the incident beam is 4.5 Å, this linewidth has no role in the broadened profile. The wave-energy-flux spectral density of the scattered $(3/2)\omega_0$ radiation follows the profile of Langmuir wave-energy-flux spectral density[2] which depends linearly on T_e and exponentially on the two plasmon convecting amplification coefficients. At high laser intensities two-plasmon instability displays saturation phenomena[31] which were not taken into account by Bychenkov *et al.*[2] Saturation of two-plasmon instability, at low levels, has also been indirectly observed in experiments by Garban *et al.*[6] and Ng and Offenberger.[32] Langdon *et al.*[33] also reported efficient saturation of the two-plasmon decay in computer simulations. As a result of the saturation mechanism the profile of Langmuir wave-energy-flux spectral density will most likely become broadened and is most probably responsible for much higher linewidths of the observed profile at higher laser intensities.

Thirdly, it is interesting to consider the peak intensity ratios of these emissions at different values of the electron temperatures [Fig. 4(b)]. For experimental values it is more reliable to consider the peak intensity ratios obtained from the values at 600, 520, and 480, respectively. Peak intensity measured at threshold has more errors in estimate because of its being very close to the background radiation. Theoretical ratios are much higher than the ratios obtained from experimental measurements. This strongly suggests involvement of serious saturation mechanisms as discussed in the previous paragraph and supports its conclusions.

Fourthly, one may consider the supplementary data obtained on aluminum and copper. It is noted that aluminum and copper have given higher peak shifts (red) of 25 Å at lower laser intensities of 1.0×10^{14} and 4.3×10^{13} W/cm^2 than that of carbon at a laser intensity of 1.5×10^{14} W/cm^2. Hydrodynamic code simulations of Turner *et al.*[10] indicate that the underdense plasma temperature is higher for the high Z targets due mainly to their lower thermal conductivity and lower hydrodynamic losses. They also believed that the increased splitting (peak to peak) observed with higher Z targets is qualitatively due to higher temperature in the plasma. The observations of Turner *et al.* are also supported qualitatively by the results of Tabatabaei and MacGowan[34] on aluminum plasma in approximately the same region of laser intensity.

Fifthly, one may consider the absence of blue-shifted emission in the present experiments. The blue wing may be generated by reflection of either the $(3/2)\omega_0$ photon or $\omega_0/2$ plasmon.[10,21,22,35] In underdense plasma experiments the reflection of $(3/2)\omega_0$ photons is impossible since there is no $9n_c/4$ surface and the reflection of the $\omega_0/2$ plasmon is small if the density gradients are very long.[21] Therefore, experimentally, one can expect only the red peak in backscatter laser plasma experiments. In some experimental situations a faint blue shift has also been reported.[36]

ACKNOWLEDGMENTS

The authors thank Dr. D. D. Bhawalkar, Head, Laser Division, Bhabha Atomic Research Centre, and Dr. V. K. Rohatgi, Head, Plasma Physics Division, Bhabha Atomic Research Centre, for constant encouragement and support.

[1]V. Yu. Bychenkov, V. P. Silin, and V. T. Tikhonchuk, Fiz. Plazmy **3**, 1314 (1977) [Sov. J. Plasma Phys. **3**, 730 (1977)].

[2]V. Yu. Bychenkov, A. A. Zozulja, V. P. Silin, and V. T. Tikhonchuk, Beitr. Plasma Phys. **23**, 331 (1983).

[3]J. L. Bobin, M. Decroisette, M. Meyer, and V. Vittal, Phys. Rev. Lett. **30**, 594 (1973).

[4]H. C. Pant, K. Eidmann, P. Sachsenmaier, and R. Sigel, Opt. Commun. **16**, 396 (1976).

[5]A. I. Avrov, V. Yu. Bychenkov, O. N. Krokhin, V. V. Dustavalov, A. A. Rupasov, V. P. Silin, G. V. Sklizkov, V. T. Tikhonchuk, and A. S. Shikanov, Zh. Eksp. Teor. Fiz. **72**, 970 (1977) [Sov. Phys.—JETP **45**, 507 (1977)].

[6]C. Garban, E. Fabre, C. Stenz, C. Popovics, J. Virmont, and F. Amiranoff, J. Phys. (Paris) Lett. **39**, L165 (1978).

[7]A. A. Offenburger, A. Ng, L. Pitt, and M. R. Cervenan, Phys. Rev. A **18**, 746 (1978).

[8]P. D. Carter, S. M. L. Sim, H. C. Barr, and R. G. Evans, Phys. Rev. Lett. **44**, 1407 (1980).

[9]K. Tanaka, L. M. Goldman, W. Seka, M. C. Richardson, J. M. Soures, and E. Williams, Phys. Rev. Lett. **48**, 1179 (1982).

[10]R. E. Turner, E. M. Campbell, P. W. Phillion, W. C. Mead, F. Ze, C. Max, G. Lasinski, and K. G. Estabrook, Lawrence Livermore National Laboratory Report No. UCRL-87218, 1982 (unpublished); R. E. Turner, D. W. Phillion, B. F. Lasinski, and E. M. Campbell, Phys. Fluids **27**, 511 (1984).

[11]E. McGoldrick and S. M. L. Sim, Opt. Commun. **39**, 172 (1981).

[12]H. Figueroa, C. Joshi, M. Azechi, N. A. Ebrahim, and K. G.

Estabrook, Phys. Fluids **28**, 1887 (1984); W. Seka, B. B. Afeyan, R. Boni, L. M. Goldman, R. W. Short, K. Tanaka, and T. W. Johnston, Phys. Fluids **28**, 2570 (1985).
[13]M. N. Rosenbluth, *ibid.* **29**, 565 (1972).
[14]I. F. Drake and Y. C. Lee, Phys. Rev. Lett. **31**, 1197 (1973).
[15]R. White, P. K. Kaw, P. Presme, M. N. Rosenbluth, G. Laval, R. Huff, and R. Varma, Nucl. Fusion **14**, 45 (1974).
[16]C. S. Liu and P. K. Kaw, in *Advances in Plasma Physics,* edited by A. Simon and W. B. Thomson (Wiley, New York, 1976), Vol. 6, p. 114.
[17]V. P. Silin and A. N. Starodub, Zh. Eksp. Teor. Fiz. **67**, 2110 (1974) [Sov. Phys.—JETP **40**, 1056 (1975)].
[18]A. P. G. Kutty and B. K. Sinha, Phys. Fluids **29**, 1298 (1986).
[19]H. C. Barr, Rutherford Laboratory Annual Report No. 022, Sec. 8.3.3, 1979 (unpublished).
[20]E. McGoldrick, S. M. L. Sim, R. E. Turner, and O. Willi, Opt. Commun. **50**, 107 (1984).
[21]V. Aboites, T. P. Hughes, E. McGoldrick, S. M. L. Sim, S. J. Kartunnen, and R. G. Evans, Phys. Fluids **28**, 2555 (1985).
[22]S. J. Kartunnen, Laser Part. Beams **3**, 157 (1965).
[23]C. S. Liu and M. N. Rosenbluth, Phys. Fluids **19**, 967 (1976).
[24]V. V. Alexandrov, Zh. Eksp. Teor. Fiz. **71**, 1826 (1976) [Sov. Phys.—JETP **44**, 958 (1976)].
[25]D. R. Nicholson, *Introduction to Plasma Theory* (Wiley, New York, 1983), p. 222.
[26]H. B. Kang, M. Waki, K. Yoshida, Y. Sakagemi, T. Yamanaka, and C. Yamanaka, J. Phys. Soc. Jpn. **34**, 504 (1973).
[27]S. Sakabe, T. Mochizuki, T. Yabe, K. Mima, and C. Yamanaka, Phys. Rev. A **26**, 2159 (1982).
[28]B. K. Sinha, J. Phys. D **13**, 1253 (1980).
[29]B. K. Sinha and N. Gopi, Phys. Fluids **23**, 1704 (1980).
[30]M. J. Herbst, P. G. Burkhalter, D. Duston, M. Emery, J. Gardner, J. Grun, S. P. Obenschain, B. H. Ripin, R. R. Whitlock, J. P. Apruzese, and J. Davis, in *Laser Interaction and Related Plasma Phenomena,* edited by H. Hora and G. H. Miley (Plenum, New York, 1984), Vol. 6, p. 329.
[31]S. J. Kartunnen, Phys. Rev. A **23**, 2006 (1981).
[32]A. Ng and A. A. Offenberger, Bull. Am. Phys. Soc. **24**, 968 (1979).
[33]A. B. Langdon, B. F. Lasinski, and W. L. Kruer, Phys. Rev. Lett. **43**, 133 (1979).
[34]S. D. Tabatabaei and B. J. MacGowan, Rutherford Appleton Laboratory Annual Report No. RAL-85-047, 1985 (unpublished), p. A1.21.
[35]J. L. Bobin, Phys. Rep. **122**, 173 (1985).
[36]J. H. Gardner, M. J. Herbst, F. C. Young, J. A. Stamper, S. P. Obenschain, C. K. Manka, K. J. Kearney, J. Grun, D. Dutson, and P. G. Burkhalter, Phys. Fluids **29**, 1305 (1986).